

Article

# Nonconventional Ca(OH)<sub>2</sub> Treatment of Bamboo for the Reinforcement of Cement Composites

Luz Adriana Sanchez-Echeverri <sup>1,2,\*</sup> , Jorge Alberto Medina-Perilla <sup>1</sup> and Eshmaiel Ganjian <sup>3</sup>

<sup>1</sup> Department of Mechanical Engineering, CIPP-CIPEM Research Group, Universidad de los Andes, Bogotá 111711, Colombia; jmedina@uniandes.edu.co

<sup>2</sup> Facultad de Ciencias Naturales y Matemáticas, Universidad de Ibagué, Carrera 22 Calle 67, Ibagué 730002, Colombia

<sup>3</sup> School of Energy, Construction and Environment, Built & Natural Environment Research Centre, Coventry University, Priory Street, Coventry CV15FB, UK; cbx111@coventry.ac.uk

\* Correspondence: luz.sanchez@unibague.edu.co; Tel.: +57-8276-0010

Received: 10 March 2020; Accepted: 15 April 2020; Published: 17 April 2020



**Abstract:** This study compares the structural and morphological changes in *Guadua angustifolia* Kunth (GAK) fiber prepared in three different ways (chips, barkless and crushed) when non-conventional alkaline treatment is applied. Moreover, it shows the improvement of mechanical properties of cement composites reinforced with these treated fibers. The three different preparations of *Guadua* were treated with a saturated solution of calcium hydroxide (5%) at 125 °C and 1.25 kPa for 3 h to remove non-cellulosic compounds. Then, their chemical, morphological, and structural properties were examined. The fibers exhibiting the higher delignification rate were selected to prepare cement composite boards, whose mechanical properties were successively compared with those of composites reinforced with untreated *G. angustifolia* fibers. The water/cement ratios of the cement mixed with the Ca(OH)<sub>2</sub>-treated and the untreated fibers were, respectively, around 0.3 and 0.25. The flexural strength and toughness of the two composites were evaluated after 7, 28, and 90 days of curing. The calcium hydroxide treatment showed higher efficiency in removing non-cellulosic materials when performed on crushed bamboo; moreover, the mechanical properties of the composites reinforced with the treated fibers were higher than those mixed with the untreated ones. After 90 days of curing, the flexural strength increased by around 40% and the toughness became three times higher ( $p < 0.05$ ). The mechanical improvement by the Ca(OH)<sub>2</sub> treatment of *G. angustifolia* fibers demonstrates its potential for the fabrication of cement composites.

**Keywords:** alkali treatment; bamboo fibers; cement composites; flexural strength; physical properties; biomass for reinforcement

## 1. Introduction

In recent years, there has been a fast rise in the use of renewable natural fibers as reinforcing agents of cement materials [1,2] in order to reduce their environmental impact. Non-wood materials are attracting growing attention due to their easy availability, low cost, rapid renewability, and eco-friendly nature [3–6]. Bamboo plants are one of the most promising sources for such materials, especially because of their abundance and rapid growth as well as their long fibers, which have superior strength properties compared with others [7,8]. *G. angustifolia* Kunth is a native bamboo of South America. It is widely utilized as a construction material due to its high mechanical resistance; however, only a part of its culm is used and the potential applications of its other parts are yet to be fully studied. Many researchers have tried to reinforce cementitious materials with bamboo fibers since they can remarkably improve the fracture toughness and flexural strength of cement composite

boards (CCBs) while simultaneously reducing their total weight [9–11]. These improvements depend mainly on the source and morphology of the fibers, the interaction at the fiber–matrix interface, the manufacturing technology, and the fiber pretreatment. All the natural fibers, including bamboo fibers, have an intrinsic hydrophilic nature, which is a drawback for a reinforcement agent since they become swollen, weakening the mechanical properties of the composite material. Thus, several chemical modifications have been tested to increase the fiber roughness and the amount of cellulose exposed on their surface [12–14].

In this viewpoint, alkali treatments are one of the major techniques adopted to obtain fibers with adequate properties for reinforcement applications due to their low cost. They can change the morphology of natural fibers by removing the impurities from their surface; for example, they can disrupt the lignin structure and break the linkage between lignin with the other carbohydrate components of lignocellulosic biomass [15]. These pretreatments provide bamboo fibers with an acceptable delignification degree as well as high yield and viscosity. Bamboo lignins generally have more phenolic hydroxyl groups than other biomass [16]. Biomass pulping is an alkali treatment method widely used in the paper industry; it is usually performed via a chemical process called Kraft pulping [17], which uses sodium hydroxide and sodium sulfide. The high pulp strength, the efficient improvement of the fiber adhesion to the cement matrix, and the ability to handle almost all species of softwood and hardwood give the Kraft process advantage over other pulping processes. However, it also has some drawbacks; for example, it requires a high pulping temperature and produces sulfur-containing volatile compounds [18].

Therefore, other alkali treatments have been considered for the production of pulp fibers with adequate properties. Among them, calcium hydroxide treatment is a useful method for selectively reducing the lignin content of lignocellulosic biomass without a significant carbohydrate loss [19,20]. Moreover, some researchers have defined it as a great option based on its cost, operation, health hazard, sustainability, and recoverability;  $\text{Ca}(\text{OH})_2$  is the least expensive per kilogram of hydroxide treatments [21]. Despite these benefits, this technique has not been fully studied as an alternative fiber pretreatment for the reinforcement of cementitious materials.

In this work, part of the GAK culm was used to prepare three different samples: chips, barkless, and crushed. These samples were treated with a calcium hydroxide solution to obtain adequate fibers to be used as reinforcement agents for cementitious materials. The treated fibers were characterized via Fourier-transform infrared spectroscopy (FTIR), X-ray diffractometry (XRD), and scanning electron microscopy (SEM). Furthermore, the effect on the flexural strength and toughness of CCBs was studied.

## 2. Materials and Methods

### 2.1. Materials

GAK is a fast-growing bamboo plant with a straight and hollow cylindrical culm, which is divided into different parts throughout its height (Figure 1).

GAK samples were taken from the internodes of the middle culm, which is the part most used for construction in Colombia and is widely commercialized, of plants grown for four years in an experimental field in La Tebaida, Quindío (central region of Colombia).

Ordinary Portland cement type I supplied by a local company was used to produce cement composites boards, the specifications of cement are summarized in Table 1.

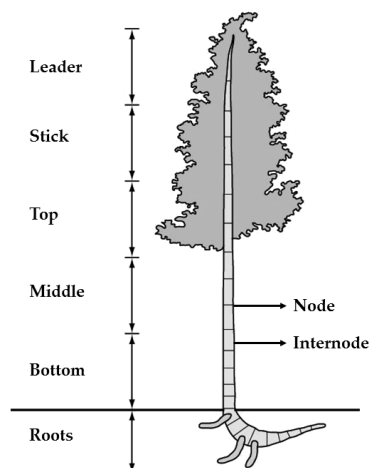


**Figure 1.** Parts of the culm of *Guadua angustifolia* Kunth.

**Table 1.** Characteristics of the ordinary Portland cement (type I), used in the composite.

Parameter	Value
Density (kg/m <sup>3</sup> )	2937
Specific surface (cm <sup>2</sup> /g)	4589.6
Unit mass (kg/m <sup>3</sup> )	825.9

## 2.2. Sample Preparation

GAK internodes were cut on a band saw machine (Shop Fox W1706, Bellingham, WA, USA) obtaining chips with approximate dimensions of (60 mm × 10 mm × 15 mm). To understand the influence of the Ca(OH)<sub>2</sub> treatment on the sample preparation, three different sample shapes were prepared from the chips obtained, and named as follows (Figure 2):

- Chips: the culm internodes were cut into small samples (60 mm × 10 mm × 15 mm);
- Barkless: the barks and internal layers of the chips were removed with a scalpel;
- Crushed: the chips were crushed in a blade mill and sieved with a 16 mesh (1.18 mm).



**Figure 2.** *G. Angustifolia* Kunth culm samples, prior to the calcium hydroxide treatment.

## 2.3. Ca(OH)<sub>2</sub> Treatment

100 g of dried samples were immersed in solutions of 5% of calcium hydroxide (Panreac®) with a liquor/sample ratio of 10:1. The solutions were cooked in an autoclave for 3 h (1 h to reach the cooking temperature of 125 °C and 2 h of cooking at 1.25 kPa). Then, the samples were washed with tap water to remove the excess Ca(OH)<sub>2</sub> solution and, finally, were air-dried for 48 h at room temperature (Figure 3).

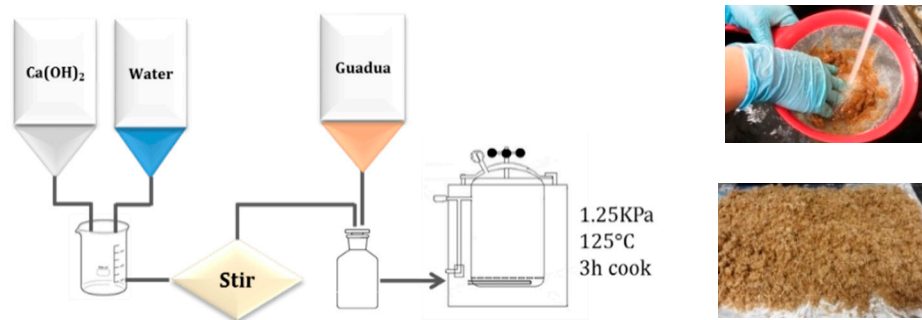


**Figure 3.** Ca(OH)<sub>2</sub> treatment process for the *G. angustifolia* samples.

#### 2.4. Fiber Surface Characterization

Scanning electronic Microscope SEM (JEOL JSM-6490LV, JEOL, Peabody, MA, USA) was used to examine the effect of the Ca(OH)<sub>2</sub> treatment on the surface of the GAK samples. The samples were cut into small pieces and attached on a carbon adhesive after being coated with a gold film to make them conductive. The observation was conducted in the low-vacuum mode at a 15 kV electron acceleration voltage and 12–20 Pa; images of different surfaces were obtained with the backscattering electron signals.

#### 2.5. Fourier Transform Infrared Spectroscopy (FTIR)

The FTIR technique was utilized to analyze the changes in the chemical structure of the GAK after the Ca(OH)<sub>2</sub> treatment. A Thermo Electron Corporation spectrometer (Nicolet 380 FT-IR, Thermo Electron Scientific Instruments LLC, Madison, WI, USA) and standard KBr pellets were used. The samples were chopped, passed through a #70 (200 μm) sieve, mixed with 300 g of KBr, and, finally, pressed into pellets (diameter of 16 mm). Five scans were performed for each sample between 400 and 4000 cm<sup>-1</sup>; the resulting spectra were analyzed with the OMNIC software (Thermo Electron Scientific Instruments LLC, Madison, WI, USA).

#### 2.6. X-Ray Diffraction

The influence of the Ca(OH)<sub>2</sub> treatment on the crystallinity of the GAK fibers was investigated with XRD. The diffraction patterns of the treated and untreated samples were recorded in the range of 4°–70° with 2θ range with a Rigaku Ultima III diffractometer (Rigaku, Tokyo, Japan) operated at 40 KV, 40 mA, and room temperature, with Cu Kα radiation (wavelength of 1.5406 Å) and a step size of 0.05 s. The Jade 9.0 software (9, KS Analytical Systemd, Aubery, TX, USA) was used for analysis. The crystallinity index (CI) was calculated according to the Segal empirical method [22] as follows (Equation (1))

$$CI(\%) = 100 \left[ \frac{(I_{002} - I_{am})}{I_{002}} \right], \quad (1)$$

where  $I_{002}$  is the maximum intensity of the (0 0 2) crystalline peak at 22°–23° and  $I_{am}$  is the minimum intensity of the peak at 18–19° [12].

#### 2.7. CCB Manufacturing

After the Ca(OH)<sub>2</sub> treatment, the sample that shows the higher variation in chemical composition according to the analyses of XRD and FTIR, was chosen as the reinforcement agent for the successive preparation of cementitious materials. The pretreated fibers (5% dry weight) were mixed with water (450 mL) and cement (130 g). The CCBs were prepared in the laboratory via a slurry vacuum de-watering technique; they were manufactured in a slab shape with a 200 mm length and a 100 mm width for the flexural test. To form and compact the boards, a 120 KN load was applied for 10 min by a compression testing machine (Avery Denison 3000, Denison Mayes Group, Hunslet, Leeds, UK).

The CCB thickness was measured before the flexural test. Once the boards were formed, they were demolded and cured at 95% humidity and 25 °C. For comparison, other CCBs were similarly produced by using untreated fibers; boards without any reinforcement agent were also fabricated as a control. The thickness of CCB was about 5 to 6 mm.

### 2.8. Water Cement Ratio of CCBs

The water/cement ratio (W/C) influences the mechanical properties of cement boards. This ratio is commonly calculated as a mass of added water divided by the cement mass; however, in the slurry method, the vacuum removes excess water, whose final water in the CCB is, therefore, different from the initial one. In this study, it was estimated after the demolding process based on the weight difference. The mass of the water retained after the manufacturing process was calculated as follows (Equation (2)):

$$\begin{aligned} w_{H_2O \text{ loss}} &= w_{total \text{ mix}} - w_{final}, \\ w_{H_2O \text{ retained}} &= 450 \text{ ml} - w_{H_2O \text{ loss}}, \end{aligned} \quad (2)$$

where  $w_{H_2O \text{ loss}}$  is the mass of water lost during the manufacturing process,  $w_{total \text{ mix}}$  is the mass of all components (water, cement, and fibers) used in the mixture, and  $w_{final}$  is the weight of the demolded CCB.

### 2.9. Flexural Strength of CCBs

A three-point loading flexural test with a 200 mm span and 5 mm/min velocity was performed according to BS EN 12467:2012 with a JJ Lloyd tensile testing machine (AMETEK Test & Calibration Instruments, Bognor Regis, Sussex, UK). To evaluate the reinforcement effect, the test was conducted on samples prepared with calcium hydroxide treated fibers, untreated fibers, and without fibers. Five samples were tested after 7, 28, and 90 days of curing (Category D); their thickness was measured at four different points and the average value was used to derive the modulus of rupture (MOR).

### 2.10. Toughness of CCBs

The toughness was evaluated by calculating the specific energy (SE) after 7, 14, and 28 days of curing through the Equation (3) [23].

$$SE = \frac{\text{Absorbed energy}}{be}, \quad (3)$$

where Absorbed energy is the integration of the stress-deflection curve between the beginning of the elastic behavior and the reduction in carrying the capacity to the maximum stress [24], and  $b$  and  $e$  are the sample width and thickness, respectively.

To compare the results on W/C, flexural strength and toughness between different samples, an analysis of variance (ANOVA) was carried out; the intervals were calculated to determine whether there were significant differences. Then, the Tukey test that is a single-step multiple comparison statistic was performed by SPSS® software (25, IBM Corp. ©, Armonk, NY, USA) to locate these differences.

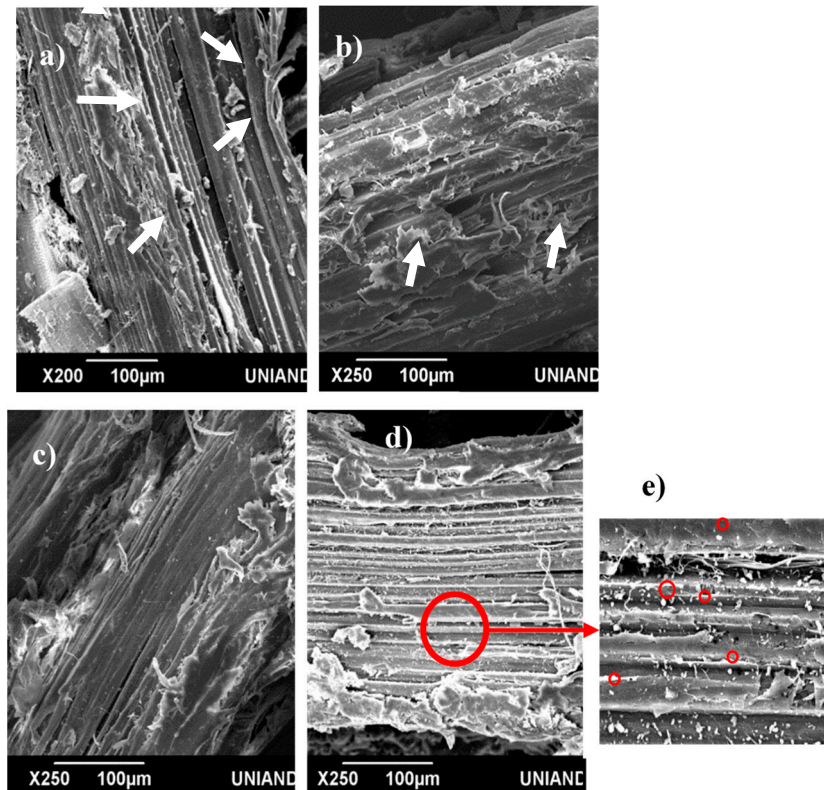
### 2.11. Fracture Surface of CCBs

SEM microscope JEOL JSM-6490LV (JEOL, Peabody, MA, USA) operated in the low-vacuum mode was used to examine the CCB fractured surface after the flexural test. The samples were cut in small pieces and attached on a carbon adhesive after being covered with a gold film to make them conductive. The analysis conditions were similar to those described in Section 2.4.

### 3. Results and Discussion

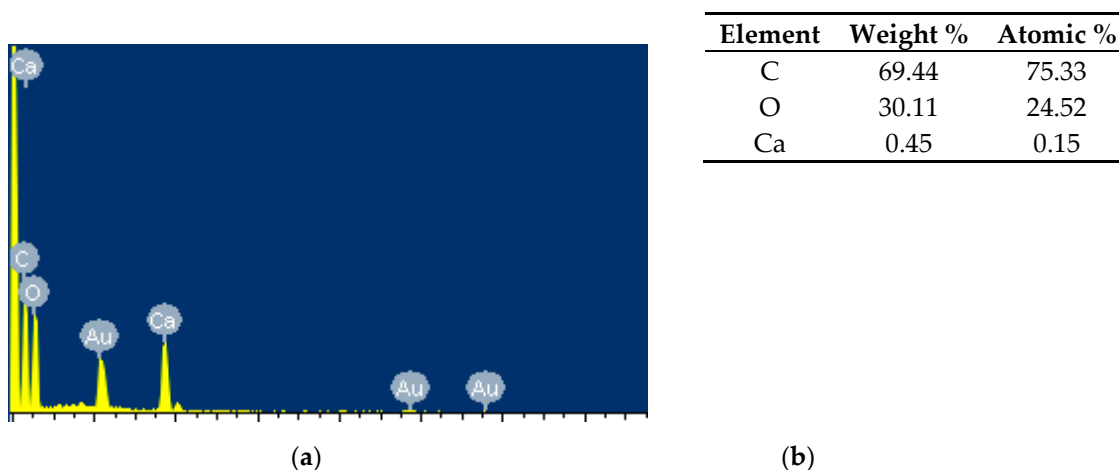
#### 3.1. $\text{Ca}(\text{OH})_2$ Treatment Effect on the Bamboo Fiber Surface Morphology

Figure 4 compares the surface of the various  $\text{Ca}(\text{OH})_2$ -treated GAK samples with that of untreated. The figure shows that impurities such as waxes and oils (arrows) present in untreated samples have been removed after  $\text{Ca}(\text{OH})_2$  treatment from the surface of the barkless and crushed samples, but it did not produce any notable modification in the chips. Over the crushed sample also showed a deposit of nodules on the surface (Figure 4e); these nodules can be associated with calcium compounds [19]; which were confirmed with EDS analysis (Figure 5).



**Figure 4.** Scanning electron microscopy images of (a) untreated and (b–e)  $\text{Ca}(\text{OH})_2$ -treated *G. angustifolia* samples: (b) chips, (c) barkless, and (d,e) crushed (the circles in (e) indicates the calcium compounds on the surface).

Figure 6 shows in more detail the surface for the barkless and crushed samples after  $\text{Ca}(\text{OH})_2$  treatment; the red arrows indicate the elementary fibrils, which were exposed by the efficient treatment with more effectiveness on the crushed surface. Binding materials such as pectin, lignins, and hemicelluloses were probably removed due to the easy penetration of the calcium ions, inducing fiber fibrillation.



**Figure 5.** (a) EDS Image of nodules observed over the crushed sample surface, (b) quantity of elements spread on the deposited nodules in the surface showed in Figure 4e.

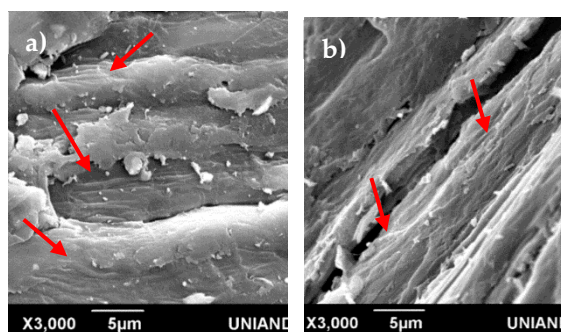


**Figure 6.** Scanning electron microscopy images of the fiber surface of the (a) barkless and (b) crushed samples after  $\text{Ca}(\text{OH})_2$  treatment.

### 3.2. FTIR Analysis of Untreated and $\text{Ca}(\text{OH})_2$ -Treated Bamboo Fibers

Figures 7 and 8 display the FTIR spectra of the samples in the  $4000\text{--}2100\text{ cm}^{-1}$  and  $2000\text{--}400\text{ cm}^{-1}$  wavenumber ranges, respectively. The band related to the presence of waxes and oils ( $2920\text{ cm}^{-1}$ ) was significantly reduced in all samples after the alkali treatment (Figure 6), which had cleaned the surface; this reduction was more noticeable on the crushed sample. The vibration band of gaseous carbon dioxide, observed at around  $2366$  and  $2341\text{ cm}^{-1}$ , was related to the background  $\text{CO}_2$  in the spectrometer; although the background was subtracted in all the spectra, those of the crushed and barkless samples still exhibited this signal due to their higher accessibility to calcium ions.

Another visible differences before and after the  $\text{Ca}(\text{OH})_2$  treatment was the modification in the band at  $1732\text{ cm}^{-1}$  (Figure 8), which is associated with the stretching of CO groups in hemicelluloses; this band almost disappeared in the crushed sample and was weaker in the barkless sample in contrast with the chips one. The signals at  $1505$  and  $1427\text{ cm}^{-1}$ , respectively related to lignin [25] and C=O vibration in carbonate ions, also decreased after the treatment. This indicates that the alkali treatment removed the non-cellulosic compounds, which is consistent with previous reports [26,27]; however, this removal was not fully effective in the studied samples since their bands could still be observed. The reduction of non-cellulosic compounds facilitates the mechanical separation of the fibers, which is beneficial for their use as reinforcement agents.

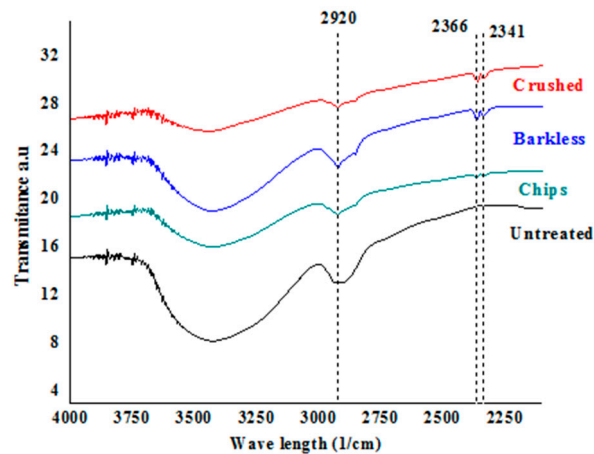


**Figure 7.** Fourier-transform infrared spectra in the 4000–2100  $\text{cm}^{-1}$  range of untreated and  $\text{Ca}(\text{OH})_2$ -treated *G. angustifolia* samples.

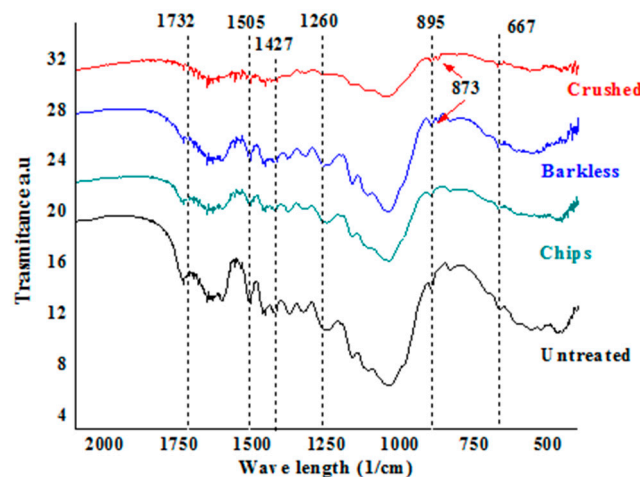


**Figure 8.** Fourier-transform infrared spectra in the 2100–500  $\text{cm}^{-1}$  range of untreated and  $\text{Ca}(\text{OH})_2$ -treated *G. angustifolia* samples.

The spectra of the crushed and barkless samples also showed a band at  $873 \text{ cm}^{-1}$ . Gunasekaran and Anbalagan have attributed this signal to calcite [28], which could be formed as a protective layer by the reaction between the carbon dioxide resulting from the carbohydrate degradation and calcium hydroxide, preventing further carbohydrate degradation [20].

### 3.3. XRD Analysis of Untreated and $\text{Ca}(\text{OH})_2$ -Treated Bamboo Fibers

Figure 9 displays the XRD patterns of the various samples investigated, along with the powder diffraction file of calcite (PDF#00-047-1743) taken from the organic material database of the Jade 9.0 software. The untreated sample exhibited a sharp, high peak at  $22.7^\circ$  and two overlapped, weaker peaks at  $15^\circ$  and  $16.3^\circ$ , attributed to cellulose I with crystallites having the preferred orientation along the fiber axis [14,29]. All the  $\text{Ca}(\text{OH})_2$ -treated samples showed diffraction patterns similar to that of the untreated one. However, in the spectra of crushed and barkless, samples an additional peak appeared at around  $29^\circ$ , which was assigned to calcite, whose presence was suggested also by the FTIR results.



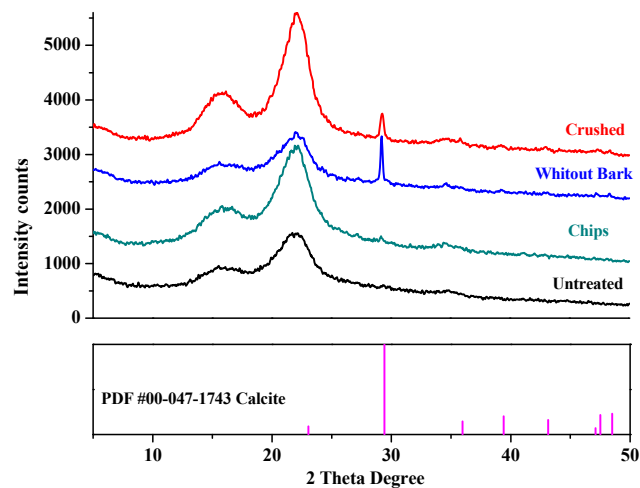


**Figure 9.** X-ray diffraction patterns of the untreated and  $\text{Ca}(\text{OH})_2$ -treated *G. angustifolia* samples, along with PDF #00-047-1743 calcite.

Alkali treatments increase the *CI* of vegetable fibers, which is related to the arrangement of the cellulosic chains. Table 2 summarizes the crystallinity indexes derived from the XRD patterns. Alkali treatments hydrolyze the amorphous parts of the cellulose in fibers, increasing the crystalline cellulose portion [30–32] which explains the *CI* increase in the samples after the  $\text{Ca}(\text{OH})_2$ -treatment. This effect was consistent with to the removal of the amorphous constituents of the fibers, such as lignins, hemicelluloses, pectin, and amorphous cellulose, as reported also by other authors [26,33].

**Table 2.** Crystallinity index (*CI*) of cellulose in the *Guadua* samples, before and after  $\text{Ca}(\text{OH})_2$  treatment.

Sample	$I_{002}$	$I_{am}$	Cellulose <i>CI</i> (%)
Untreated	1557	829	46.8
<i>Guadua</i> chips	2419	1085	55.1
Barkless <i>Guadua</i>	1487	782.5	47.4
Crushed <i>Guadua</i>	2908	1009	65.3

However, the essential peaks of the GAK fibers were not shifted after the treatment, which indicates that there was no transition from cellulose I into cellulose II and the relative carbohydrates were not significantly altered [14,34]. Therefore, the *CI* variations originated only from the elimination of amorphous compounds such as lignins and hemicelluloses.

### 3.4. *W/C* of CCBs

Based on the results of fibers after alkaline treatment, crushed samples were selected to manufacture due to the efficiency of calcium treatment in this sample.

The *W/C* influences the strength of a composite. *W/C* is generally defined as the ratio between the initial cement and water weights used for the mixture [35]. With the same *W/C*, the addition of steel fibers significantly improves the compressive strength of concrete after 28 days [36]. However, in the slurry method, the vacuum process removes excess water, whose final water in the CCB is, therefore, different from the initial one. Table 3 lists the average *W/C* values measured for CCBs reinforced with  $\text{Ca}(\text{OH})_2$ -treated and untreated fibers and for those without fibers, indicating that the fiber inclusion increased the *W/C* with more intensity in the treated calcium fibers. It was coherent with the water retention capacity of the fibers. The Tukey test ( $p < 0.05$ ) showed a significant difference on the *W/C* ratio for all CCB.

**Table 3.** Water/cement ratios (W/C) of different composite cement boards (CCB).

CCB type	W/C
Without fibers	0.17 ± 0.01
With untreated fibers	0.23 ± 0.03
With Ca(OH) <sub>2</sub> -treated fibers	0.27 ± 0.01

3.5. Mechanical Properties of CCBs

Figure 10 shows the load-extension curves of the flexural strength test of different composites. Table 4 summarizes the MOR and SE of the various CCBs after 7, 28, and 90 days of curing. In all the cases, the MOR increased along with the curing time, while the SE did not significantly change.

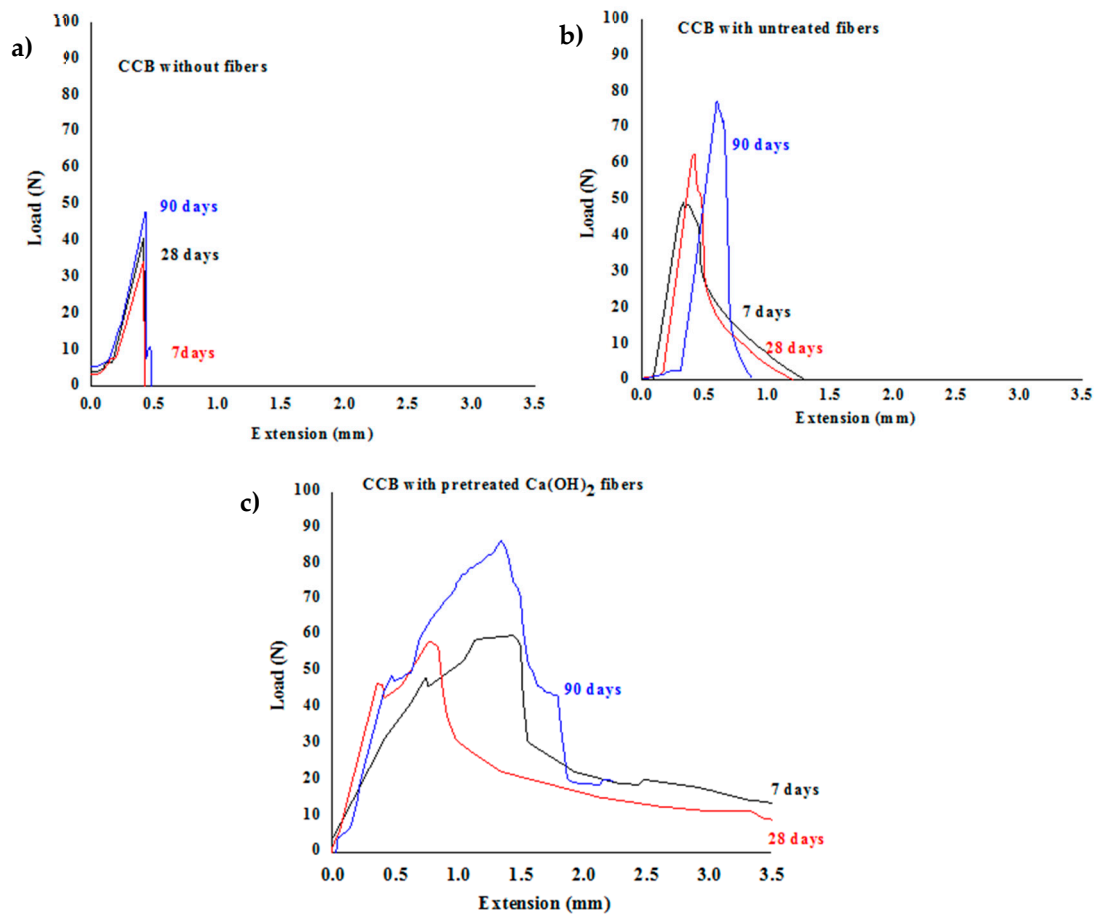


**Figure 10.** Load–extension curve of various composite cement boards (CCBs) after 7, 28, and 90 days of curing (a) CCB without fibers, (b) CCB with untreated fibers, and (c) CCB with calcium treated fibers.

**Table 4.** Average Modulus of Rupture (MOR) and Specific Energy (SE) of various composite cement boards (CCBs) after 7, 28, and 90 days of curing.

CCB Reinforcement	MOR (MPa)			Specific Energy (kJ/m <sup>2</sup> )		
	7 days	28 days	90 days	7 days	28 days	90 days
Unreinforced	4.8 ± 0.9 <sup>a</sup>	5.2 ± 0.6 <sup>a</sup>	5.6 ± 0.9 <sup>a</sup>	0.19 ± 0.02 <sup>a</sup>	0.20 ± 0.01 <sup>a</sup>	0.25 ± 0.02 <sup>a</sup>
Untreated fibers	3.6 ± 0.9 <sup>b</sup>	5.0 ± 0.9 <sup>a</sup>	7.4 ± 0.5 <sup>b</sup>	0.63 ± 0.03 <sup>b</sup>	0.51 ± 0.02 <sup>b</sup>	0.61 ± 0.02 <sup>b</sup>
Ca(OH) <sub>2</sub> -treated fibers	5.2 ± 0.8 <sup>a</sup>	5.4 ± 0.6 <sup>a</sup>	8.2 ± 0.9 <sup>b</sup>	1.19 ± 0.20 <sup>c</sup>	0.99 ± 0.09 <sup>c</sup>	1.09 ± 0.10 <sup>c</sup>

The same letter in the column means results do not differ by the Tukey Test ( $p < 0.05$ ).

The use of GAK fibers improved the flexural strengths of the CCBs. The highest variation with curing time was exhibited by the CCB reinforced with untreated fibers, which increased from 3.6 to 7 days up to 7.4 MPa and over 100% after 90 days. For the CCB reinforced with  $\text{Ca}(\text{OH})_2$ -treated fibers, this increase reached 57% varying from 5.2 MPa after 7 days to 8.2 MPa after 90 days. In the unreinforced CCB, there was no significant difference during time, with a variation of only around 15% from 4.8 after 7 days up to 5.6 MPa after 90 days. Although the CCB reinforced with untreated fibers showed the highest variation, it did not reach the highest flexural value after 90 days. This was due, as mentioned before, to the fact that, during the first days, the water-soluble extractives in the fibers were released through the contact between untreated fibers and the alkaline medium of the cement, preventing the hydration of the cement core grains and, thus, retarding the cement setting, which resulted in a low flexural strength in the initial days. As the curing time increased, the fibers without extractives had more hydrogen active site to anchorage with cement grains, increasing significantly the flexural strength. Moreover, the roughness of the fibers after the  $\text{Ca}(\text{OH})_2$  treatment, revealed by the SEM images, provided mechanical anchorage, which led to higher MOR values. It has been reported the improvement of the mechanical performance of CCBs with the inclusion of alkali-treated fibers. The values for MOR of these composites are related to the source of fiber and the used alkaline treatment. For bamboo fibers treated with sodium hydroxide, the most alkaline treatment used, CCBs shows flexural strength between 5 MPa to 12 MPa [37]. However, bamboo fibers treated with less environmental impact treatments, such as organosolv pulp, CCBs show maximum flexural stress of 8 MPa [38]. The mechanical results obtained with calcium hydroxide treatment demonstrate the potential of this treatment as an alternative to process *Guadua* in cement-based composites.

The flexural strength exhibited a non-conventional behavior in relation to the W/C. A lower W/C commonly leads to a higher strength; however, the CCB reinforced with the fibers with highest W/C, showed also higher flexural strength. This trend could be due to the swelling capacity of the  $\text{Ca}(\text{OH})_2$ -treated fibers, which absorbed water during the mixing and successively released it during the curing, enhancing the water diffusion and the cement hydration, as reflected in the high flexural strength.

Upon analyzing the SE values, it was observed that the energy absorption was higher in the CCB reinforced with  $\text{Ca}(\text{OH})_2$ -treated fibers in the three curing stages; this might be related to the fiber surface modification by the alkali treatment, which resulted in less rigid fibers.

The Tukey test results for the MOR and SE after 7, 28, and 90 days of curing corresponded to three independent replicates per each mixture. After seven days, the MOR of the CCB reinforced with untreated fibers statistically differed ( $p < 0.05$ ) from those of the other two samples; this could be due to the presence of extractives and non-cellulosic compounds in the untreated fibers, which delayed the cement hydration [39]. After 90 days, the MOR of both the reinforced CCBs were statistically different ( $p < 0.05$ ) from that of the unreinforced one, indicating the positive effect of the reinforcement. On the other hand, at every curing stage, all the samples exhibited statistically different specific energies ( $p < 0.05$ ) from each other.

The flexural results for the CCB reinforced with calcium  $\text{Ca}(\text{OH})_2$ -treated fibers showed a flexural strength suitable for fiber–cement flat sheets class 2 categories C and D, according to BS EN 12467:2012 [40], which are intended for internal applications, where they may be subjected to heat and moisture but not to frost.

### 3.6. Fracture Surface of CCBs

After the flexural test, the fracture surfaces of the broken CCBs reinforced with fibers were observed by SEM to determine the main fiber failure mechanism (Figure 11). In the sample with untreated fibers, the fibers were fractured after the composite failure (Figure 11a,b); this mechanism is associated with a disruption of energy dissipation and weaker fibers, resulting in worse mechanical behavior. In the composite reinforced with  $\text{Ca}(\text{OH})_2$ -treated fibers, the surface modification by the alkali treatment provided fiber with better mechanical characteristics avoiding fracture. Thus, the fibers suffered pull

out (Figure 11c,d) during the fracturing, allowing energy dissipation and, hence, endowing the CCB with a better mechanical performance. This fiber behavior into cement composite is reflected in the mechanical performance of CCB; where CCB reinforced with alkali-treated fibers showed the highest toughness and flexural strength. The performance on the fiber mechanical failure is attributed to the surface differences arising from the alkaline treatment [41].

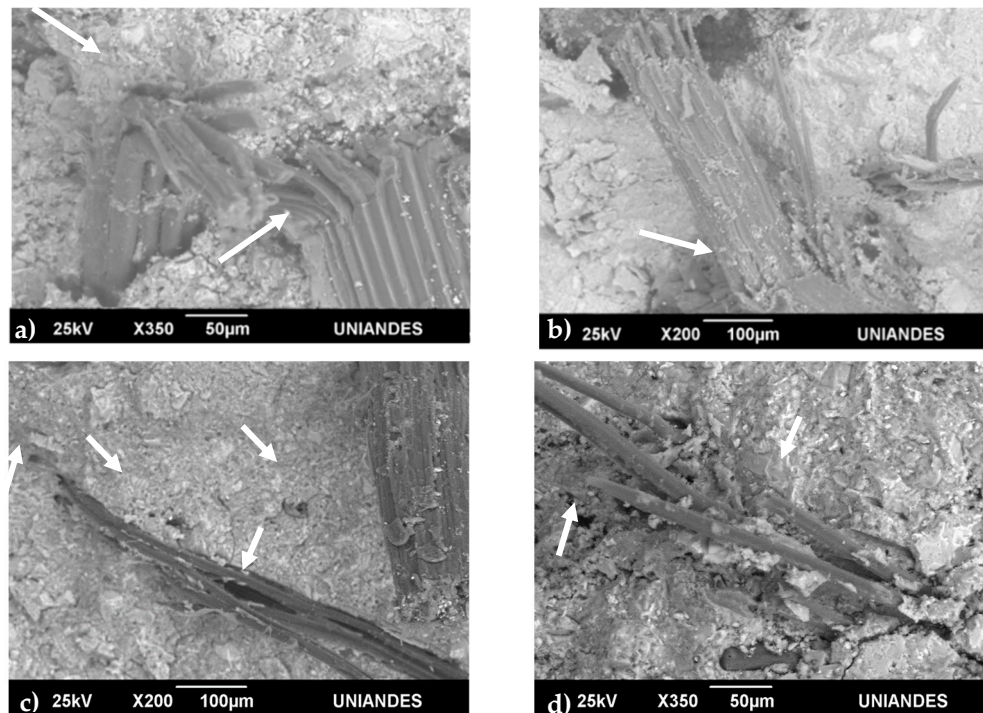


**Figure 11.** Scanning electron microscopy images of the fracture surfaces of composite cement boards reinforced with (a,b) untreated and (c,d)  $\text{Ca}(\text{OH})_2$ -treated *G. angustifolia* fibers, after (a,c) 7 and (b,d) 28 days.

The CCB reinforced with untreated fibers showed a prominent loss in bonding since the *G. angustifolia* fibers shrank strongly upon drying during curing.

Matrix cracking also occurred near the fibers, in both samples, because of the internal tensile stress generated by the fiber volume variation.

#### 4. Conclusions

The calcium hydroxide treatment affected the surface and structure of all the *G. angustifolia* samples. It successfully removed the hemicelluloses and lignins from the fibers and disrupted the cell wall structure, increasing the cellulose crystallinity. Moreover, this alkali treatment was more efficient removing the non-cellulosic materials in the crushed sample compared with chips and barkless samples.

The mechanical properties of the CCB reinforced with  $\text{Ca}(\text{OH})_2$ -treated fibers, determined via modulus of rupture and toughness were higher than reinforced with untreated fibers and the unreinforced one ( $p < 0.05$ ). This proves the efficiency of the  $\text{Ca}(\text{OH})_2$  treatment of bamboo fibers for CCB production.

**Author Contributions:** Conceptualization, L.A.S.-E.; Formal analysis, L.A.S.-E.; Investigation, L.A.S.-E. and J.A.M.-P.; Methodology, L.A.S.-E., J.A.M.-P., and E.G.; Project administration, J.A.M.-P.; Supervision, J.A.M.-P., and E.G.; Writing—original draft, L.A.S.-E.; Writing—review & editing, L.A.S.-E., J.A.M.-P., and E.G. All authors have read and agreed to the published version of the manuscript.

**Funding:** This research received no external funding.

**Acknowledgments:** L.A Sanchez would like to thank COLCIENCIAS for its financial support for PhD study. The authors appreciate technical support in the laboratory procedures provided by laboratory staff at Universidad de los Andes and Coventry University.

**Conflicts of Interest:** The authors declare no conflict of interest.

## References

1. Santos, S.F.; Tonoli, G.H.D.; Mejia, J.E.B.; Fiorelli, J.; Savastano, H., Jr. Non-conventional cement-based composites reinforced with vegetable fibers: A review of strategies to improve durability. *Mater Constr.* **2015**, *65*, 1–20.
2. Johnston, C. *Fiber—Reinforced Cements and Concretes*; CRC Press-Taylor & Francis Group: New York, NY, USA, 2010; p. 370.
3. Liu, R.; Luo, S.; Cao, J.; Chen, Y. Mechanical properties of wood flour/poly (lactic acid) composites coupled with waterborne silane-polyacrylate copolymer emulsion. *Holzforschung* **2016**, *70*, 439–447. [[CrossRef](#)]
4. Khorami, M.; Ganjian, E. Comparing flexural behaviour of fibre–cement composites reinforced bagasse: Wheat and eucalyptus. *Constr. Build. Mater.* **2011**, *25*, 3661–3667. [[CrossRef](#)]
5. Khorami, M.; Ganjian, E. The effect of limestone powder, silica fume and fibre content on flexural behaviour of cement composite reinforced by waste Kraft pulp. *Constr. Build. Mater.* **2013**, *46*, 142–149. [[CrossRef](#)]
6. Monteiro, S.N.; Lopes, F.P.D.; Barbosa, A.P.; Bevitori, A.B.; DaSilva, I.L.A.; DaCosta, L.L. Natural Lignocellulosic Fibers as Engineering Materials—An Overview. *Metall. Mater. Trans. A* **2011**, *42*, 2963–2974. [[CrossRef](#)]
7. Osorio, L.; Trujillo, E.; Van-Vuure, A.W.; Verpoest, I. Morphological aspects and mechanical properties of single bamboo fibers and flexural characterization of bamboo/ epoxy composites. *J. Reinf. Plast. Comp.* **2011**, *30*, 396–408. [[CrossRef](#)]
8. Yu, Y.; Tian, G.; Wang, H.; Fei, B.; Wang, G. Mechanical characterization of single bamboo fibers with nanoindentation and microtensile technique. *Holzforschung* **2011**, *65*, 113–119. [[CrossRef](#)]
9. Abdul Khalil, H.P.S.; Bhat, I.U.H.; Jawaid, M.; Zaidon, A.; Hermawan, D.; Hadi, Y.S. Bamboo fibre reinforced biocomposites: A review. *Mater. Des.* **2012**, *42*, 353–368. [[CrossRef](#)]
10. Tolosa, R.A.; Jimenez-Obando, G.; Arias, N.P.; Cardona, C.A.; Giraldo, O. Cementitious Materials Reinforcement Using *Angustifolia kunth* Bamboo Fiber Covered with Nanostructured Manganese Oxide. *Ind. Eng. Chem. Res.* **2014**, *53*, 8452–8463. [[CrossRef](#)]
11. Bentur, A.; Mindess, S. *Fibre Reinforced Cementitious Composites*; Taylor & Francis Group: New York, NY, USA, 2007; p. 595.
12. Cai, M.; Takagi, H.; Nakagaito, A.N.; Li, Y.; Waterhouse, G.I.N. Effect of alkali treatment on interfacial bonding in abaca fiber-reinforced composites. *Compos. Part A Appl. S* **2016**, *90*, 589–597. [[CrossRef](#)]
13. Alessandra, F.; Panthapulakkal, S.; Konar, S.; Sain, M.; Bufalino, L.; Raabe, J.; De Andrade, I.P.; Martins, M.A.; Tonolii, G.H.D. Improving cellulose nanofibrillation of non-wood fiber using alkaline and bleaching pre-treatments. *Ind. Crop. Prod.* **2019**, *131*, 203–212.
14. Chen, H.; Yu, Y.; Zhong, T.; Wu, Y. Effect of alkali treatment on microstructure and mechanical properties of individual bamboo fibers. *Cellulose* **2016**, *24*, 333–347. [[CrossRef](#)]
15. Bajpai, P. Pretreatment of Lignocellulosic Biomass. In *Pretreatment of Lignocellulosic Biomass for Biofuel Production*; Sharma, S., Ed.; Springer: Singapore, 2016; p. 87.
16. Salmela, M.; Alén, R.; Vu, M.T.H.; Thi, A.; Vu, H. Description of kraft cooking and oxygen–alkali delignification of bamboo by pulp and dissolving material analysis. *Ind. Crop. Prod.* **2008**, *28*, 47–55. [[CrossRef](#)]
17. Pacheco-Torgal, F.; Jalali, S. Cementitious building materials reinforced with vegetable fibres: A review. *Constr. Build. Mater.* **2011**, *25*, 575–581. [[CrossRef](#)]
18. Gierer, J. Chemical aspects of Kraft pulping. *Wood Sci. Technol.* **1980**, *14*, 241–266. [[CrossRef](#)]
19. Anggono, J.; Sugondo, S.; Henrico, S.; Purwaningsih, H. Effect of Alkali Treatment Using Calcium Hydroxide and the Fiber Length on the Strength of Sugarcane Bagasse Fibers-Polypropylene Composites. *Appl. Mech. Mater.* **2015**, *815*, 106–110. [[CrossRef](#)]
20. Sierra, R.; Granda, C.B.; Holtzapple, M.T. Lime Pretreatment. In *Biofuels*; Mielenz, J.R., Ed.; Humana Press: Totowa, NJ, USA, 2009; pp. 115–124.

21. Chang, V.S.; Nagwani, M.; Kim, C.H.; Holtzapfle, M.T. Oxidative Lime Pretreatment of High-Lignin Biomass. *Appl. Biochem. Biotechnol.* **2001**, *94*, 1–28. [[CrossRef](#)]
22. Segal, L.; Creely, J., Jr.; Martin, A.E.J.; Conrad, C.M. An Empirical Method for Estimating the Degree of Crystallinity of Native Cellulose Using the X-Ray Diffractometer. *Text. Res. J.* **1959**, *29*, 786–794. [[CrossRef](#)]
23. Jarabo, R.; Fuente, E.; Monte, M.; Savastano, H., Jr.; Mujt e, P.; Negro, C. Use of cellulose fibers from hemp core in fiber-cement production. Effect on flocculation, retention, drainage and product properties. *Ind. Crop. Prod.* **2012**, *39*, 89–96. [[CrossRef](#)]
24. Rusu, M.; M rseburg, K.; Gregersen,  .; Yamakawa, A.; Liukkonen, S. Relation Between Fibre Flexibility and Cross Sectional Properties. *BioResources* **2011**, *6*, 641–655.
25. Rodrigues, J.; Faix, O.; Pereira, H. Determination of Lignin Content of Eucalyptus globulus Wood Using FTIR Spectroscopy. *Holzforschung* **1998**, *52*, 46–50. [[CrossRef](#)]
26. Le Trodec, M.; Sedan, D.; Peyratout, C.; Bonnet, J.P.; Smith, A.; Guinebretiere, R.; Gloaguen, V.; Krauszc, P. Influence of various chemical treatments on the composition and structure of hemp fibres. *Compos. Part A Appl. S* **2008**, *39*, 514–522. [[CrossRef](#)]
27. Yuan, Z.; Kapu, N.S.; Beatson, R.; Martinez, D.M.; Feng, X. Effect of alkaline pre-extraction of silica and hemicellulose on Kraft pulping of bamboo. *Ind. Crop. Prod.* **2016**, *91*, 1–41. [[CrossRef](#)]
28. Gunasekaran, S.; Anbalagan, G. Spectroscopic characterization of natural calcite minerals. *Spectrochim. Acta A* **2007**, *68*, 656–664. [[CrossRef](#)] [[PubMed](#)]
29. Liu, Y.; Hu, H. X-ray diffraction study of bamboo fibers treated with NaOH. *Fiber Polym.* **2008**, *9*, 735–739. [[CrossRef](#)]
30. Ferreira, S.R.; Silva, F.D.A.; Lima, P.R.L.; Toledo Filho, R.D. Effect of fiber treatments on the sisal fiber properties and fiber-matrix bond in cement based systems. *Constr. Build. Mater.* **2015**, *101*, 730–740. [[CrossRef](#)]
31. Heise, K.; Rossberg, C.; Str tz, J.; B urich, C.; Brendler, E.; Keller, H.; Fischer, S. Impact of pre-treatments on properties of lignocelluloses and their accessibility for a subsequent carboxymethylation. *Carbohydr. Polym.* **2017**, *161*, 82–89. [[CrossRef](#)]
32. Wang, X.; Chang, L.; Shi, X.; Wang, L. Effect of Hot-Alkali Treatment on the Structure Composition of Jute Fabrics and Mechanical Properties of Laminated Composites. *Materials* **2019**, *12*, 1386. [[CrossRef](#)]
33. Faruk, O.; Bledzki, A.K.; Fink, H.; Sain, M. Progress in Polymer Science Biocomposites reinforced with natural fibers: 2000–2010. *Prog. Polym. Sci.* **2012**, *37*, 1552–1596. [[CrossRef](#)]
34. Boufi, S.; Chaker, A. Easy production of cellulose nanofibrils from corn stalk by a conventional high speed blender. *Ind. Crop. Prod.* **2016**, *93*, 39–47. [[CrossRef](#)]
35. Gao, D.; Zhang, L.; Nokken, M.; Zhao, J. Mixture Proportion Design Method of Steel Fiber Reinforced Recycled Coarse Aggregate Concrete. *Materials* **2019**, *12*, 375. [[CrossRef](#)] [[PubMed](#)]
36. Saidani, M.; Saraireh, D.; Gerges, M. Behaviour of different types of fibre reinforced concrete without admixture. *Eng. Struct.* **2016**, *113*, 328–334. [[CrossRef](#)]
37. Xie, X.; Zhou, Z.; Yan, Y. Flexural properties and impact behaviour analysis of bamboo cellulosic fibers filled cement based composites. *Constr. Build. Mater.* **2019**, *241*, 403–414. [[CrossRef](#)]
38. Potential of bamboo organosolv pulp as a reinforcing element in fiber–cement materials in fiber–cement materials. *Constr. Build. Mater.* **2014**, *72*, 65–71. [[CrossRef](#)]
39. Wei, J.; Meyer, C. Degradation mechanisms of natural fiber in the matrix of cement composites. *Cem. Concr. Res.* **2015**, *73*, 1–16. [[CrossRef](#)]
40. CEN. BS EN 12467:2004 Fibre-Cement Flat Sheets—Product Specification and Test Methods. 2004.
41. Klerk, M.D.; Kayondo, M.; Moelich, G.M.; De Villers, W.I.; Combrinck, R. Durability of chemically modified sisal fibre in cement-based composites. *Constr. Build. Mater.* **2020**, *241*, 117835. [[CrossRef](#)]

